Applying Digital Image Correlation to Biological Materials

Joel D. Krehbiel
Senior in Mathematics and Physics, Bethel College

Thomas A. Berfield
Graduate Assistant in Theoretical and Applied Mechanics, UIUC

Advisors: TAM Prof. Nancy R. Sottos and AE Prof. John Lambros

Digital image correlation has become a common method for determining mechanical properties of rigid engineering materials. By comparing digital images of the material before and after deformation, strain and displacement response can be determined. In the current work, we expand this method for use on soft biological materials, in particular skin. Specifically, we show that digital image correlation can be used to determine mechanical properties of skin under different conditions, including displacement, uniaxial tension, and elevated temperature.

Introduction

Digital image correlation

Digital imaging techniques allow computation of displacements and displacement gradients by comparing images before and after deformation. A random speckle pattern is produced on the surface to be imaged. A digital image—a discrete record of light-intensity levels—is gathered during deformation. In use of the digital image correlation (DIC) technique, one assumes that the speckle pattern imaged before deformation is related to the speckle pattern after deformation by rigid-body motion and applied strains. As shown in Fig. 1, a particular point (x, y) has a light-intensity value $f(x, y)$ before deformation, and this point maps to a particular point (x^*, y^*) with intensity $f^*(x^*, y^*)$ in the deformed image. These relations can be expressed as

$$x^* = x + u + \frac{\partial u}{\partial x}\Delta x + \frac{\partial u}{\partial y}\Delta y\,, \quad y^* = y + v + \frac{\partial v}{\partial x}\Delta x + \frac{\partial v}{\partial y}\Delta y\,. \tag{1}$$

Here, u and v are the displacements in the x and y directions, respectively. The terms $\partial u/\partial x$ and $\partial v/\partial y$ correspond to normal strains in the x and y directions, respectively. Finally, $\partial u/\partial y$ and $\partial v/\partial x$ contribute to shear strain [1].

To determine these displacements and displacement gradients, one must minimize a correlation coefficient. Typically, the least-squares method is used to define the correlation coefficient as

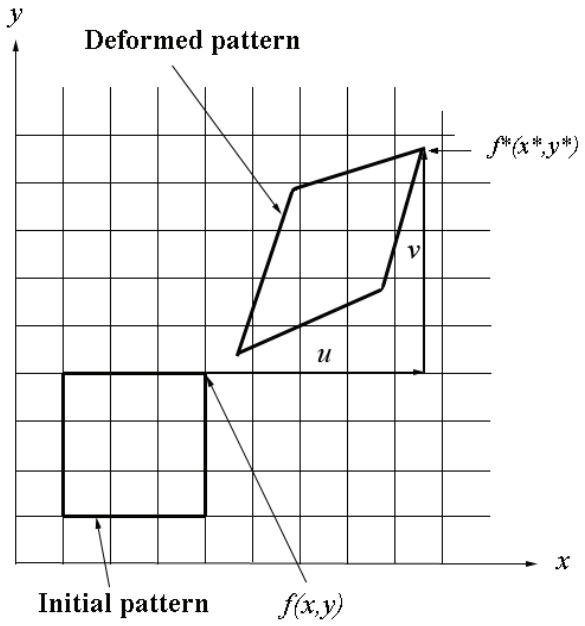

Fig. 3. Displacement components of a deformed pattern as a function of the components of the undeformed body.

$$C = \int_{\Delta M} \left(f(x,y) - f^*(x^*,y^*) \right)^2 \mathrm{d}x\mathrm{d}y \,, \tag{2}$$

where ΔM is the pattern surface [2]. Digital image correlation allows for quick minimization of this coefficient; thus displacement and displacement gradients can easily be determined.

Mechanical properties of skin

The third largest organ in our bodies, skin plays the important role of a barrier between internal organs and the external world. Skin is composed of three layers: the outer epidermal layer, the dermis, and the inner layer of subcutaneous fat. The dermis consists of a heterogeneous mix of collagen fibrils and elastin fibers in a proteoglycan matrix [3].

In previous studies on the mechanical properties of skin, tensile tests have been commonly used to determine such properties as Young's modulus, tensile strength, ultimate modulus of elasticity, and ultimate strain. Data obtained from tensile tests show a consistent stress–strain curve for skin. As the load is applied, the collagen fibrils in the skin align and the skin reacts elastically. Then the curve exhibits roughly exponential behavior until the skin reacts elastically right before rupture [4].

Researchers have also sought to find a suitable simulant for human skin. Pigskin reacts similar to human skin, without requiring the special handling of human skin. Earlier works have shown the stress at failure for pigskin to be 15 MPa for pig back skin, comparable with the values of 5 to 30 MPa measured for human skin. Additionally, the ultimate strain for pigskin ranges from 25 to 118%, similar to values of 35 to 115% that have been found for human skin [4, 5]. Additionally, pig back skin shows little directionally dependent response, making it most suitable for testing. Thus pig back skin can suitably simulate the mechanical response of human skin.

Scope of work

Here we attempt to apply digital imaging techniques to measure the deformation of pigskin. The main focus of the research dealt with determining the appropriate speckling technique, testing the translation limits of our DIC software, and measuring stress and strain applied to skin. We also sought to determine mechanical response differences of skin that is heated, potentially to help burn victims.

Material and methods

Pig back skin was obtained from the Animal Sciences Department at the University of Illinois at Urbana-Champaign. To keep the skin fresh, we sealed the samples in freezer bags and froze them, as this procedure has been shown to maintain most mechanical properties of skin [6]. After removing the inner fat layer and the outer epidermis and hair using a razor blade and scalpel, we cut samples approximately 15 by 35 mm from the dermis.

Several methods were tried to produce the appropriate speckle pattern on the skin. Marcellier et al. suggested that skin may be naturally featured enough to have a random pattern of its own [2]. Additionally, spray-painting has been used to produce speckle patterns in other DIC experiments [7]. Finally, we hypothesized that staining the skin with a fluorescent dye would bring out a random pattern. We prepared samples by air-brushing them with ink, staining them with a solution of fluorescent Rhodamine and water, or leaving them unaltered. As a control, we air-brushed a sheet of paper to test the accuracy and precision of our DIC software. Samples were glued to microscope slides using cyanoacrylate cement. Images were taken before and after a simple unidirectional rigid-body translation to determine if each method provided a sufficient pattern for correlation.

To provide the translations, a DC voltage was applied to a calibrated piezoelectric actuator. The imaging setup involved a QImaging Retiga monochrome CCD camera with 1280 by 1024 pixel resolution mounted on a Leica DM4 optical microscope. The spatial resolution of 2.10 microns per pixel provided a field of view of 2680 by 2150 microns. Images of the sample were acquired before and after deformation.

For uniaxial tension tests a different setup was required. Specimens were cut using an electric food slicer to provide a flat surface for correlation. The samples were then cut to size using a razor blade. Final specimen dimensions were approximately 2 mm thick by 7 mm wide by 35 mm long. To increase the friction between the grips and the skin and to minimize strain concentration at the grips, glass–epoxy circuit-board end-tabs were glued to each end of the sample using cyanoacrylate cement. In order to provide a speckle pattern for correlation, we air-brushed half the samples with ink. The others were placed in the Rhodamine dye solution to produce the effect.

The effects of heat on skin were investigated by placing samples in boiling water for various lengths of time. Some samples were left untreated, while others were immersed for 30, 60, or 120 s.

Figure 2 shows the tension test setup. A servo-actuator (PI Model M-224.50), load cell (Sensotec, 50 lb), and synchronized image acquisition were controlled by a LabVIEW (National Instruments) program. The samples were gripped between two small metal plates using two

machine screws on each end. Images were captured in real time every two seconds as the samples were stretched at the loading rate of 0.01 mm/sec.

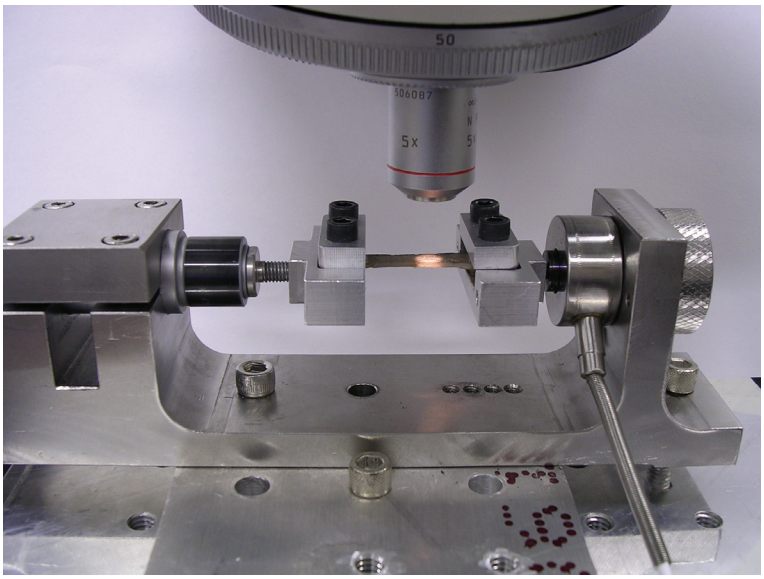

Fig. 2. Tension test setup. The servo-actuator on the left provided the tension, while the load cell on the right measured the load on the sample. The microscope allowed images to be taken for DIC use.

Results and discussion

Rigid-body translation

We performed translation tests on paper, Rhodamine-dyed skin, and air-brushed skin. Plain skin did not have a sufficient natural speckle pattern to correlate, so no correlations were attempted for plain skin. The DIC software produced vector fields similar to that shown in Fig. 3. From the data, we determined the average vector displacement. We compared these vector displacements with the known applied translations. Figure 4 displays the results.

As expected, the paper samples correlated very well, even at the smallest translations we provided. However, for the samples painted with ink, the data become anomalous at translations below one micron. At 0.14 microns (0.07 pixels), the measured translations for the spray-painted samples do not correspond to the applied translations. This result is to be expected, as the precision of DIC has been found to be around 0.1 pixels [8]. However, the samples dyed in Rhodamine appear to correlate well even at the smallest translations provided. Results demonstrate the capability of the DIC method on skin for translations greater than 0.2 microns.

Tensile tests

From the data gathered during the tensile tests, we calculated stress using the load cell and specimen dimension and calculated strain from the actuator displacement. Our results are shown in Fig. 5. The curves exhibit the characteristic initial elongation, followed by a roughly exponential increase. The results indicate the heat treatments had a significant effect on the material response. The samples placed in boiling water show a clear loss of stiffness (the slope of the curve). As the time spent at elevated temperature increased, the samples became less stiff.

However, it appears that there was no loss in stiffness between the 60 s and 120 s samples. Once the samples reach a critical time period at elevated temperature, they seem to react similarly.

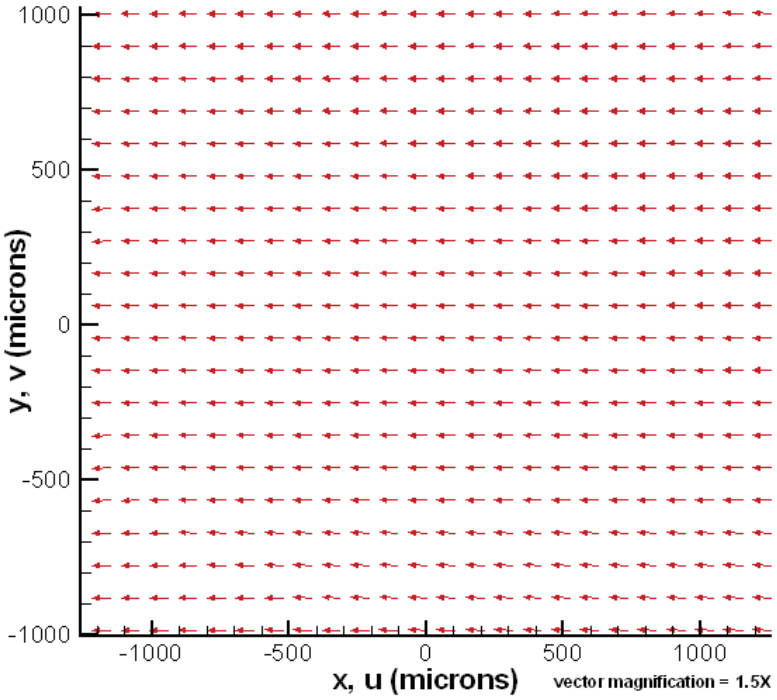

Fig. 3. Sample vector plot of DIC data taken from a uniform translation of 11.7 microns to the left. Sample was dyed with Rhodamine.

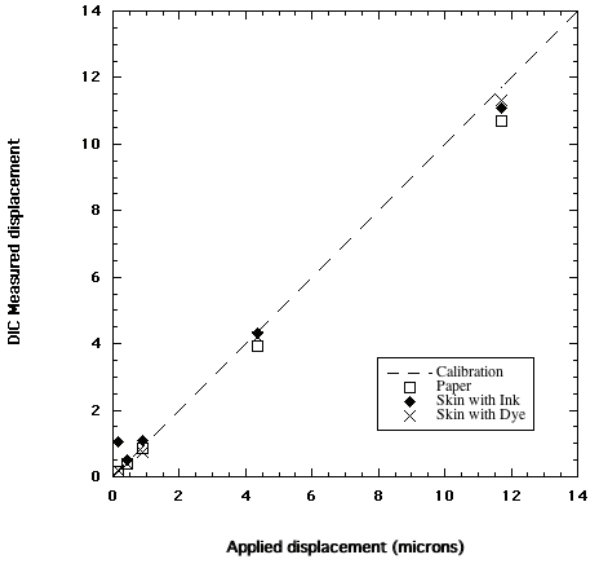

(a) Translations smaller than 14 microns

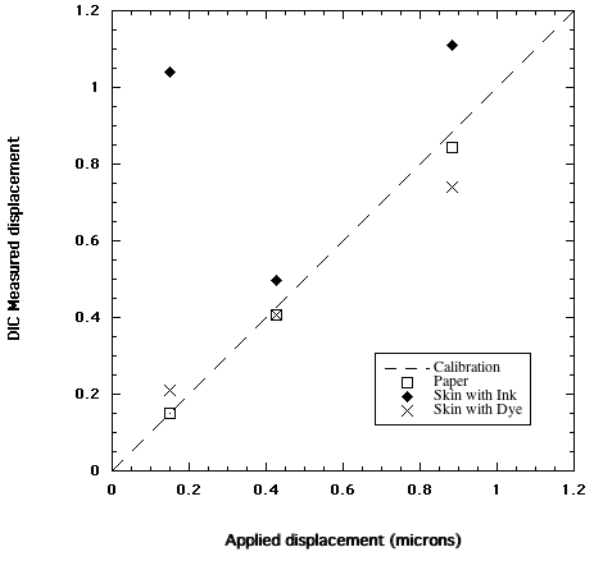

(b) Translations smaller than 1.2 microns

Fig. 4. Comparison of DIC results with output of piezoelectric actuator.

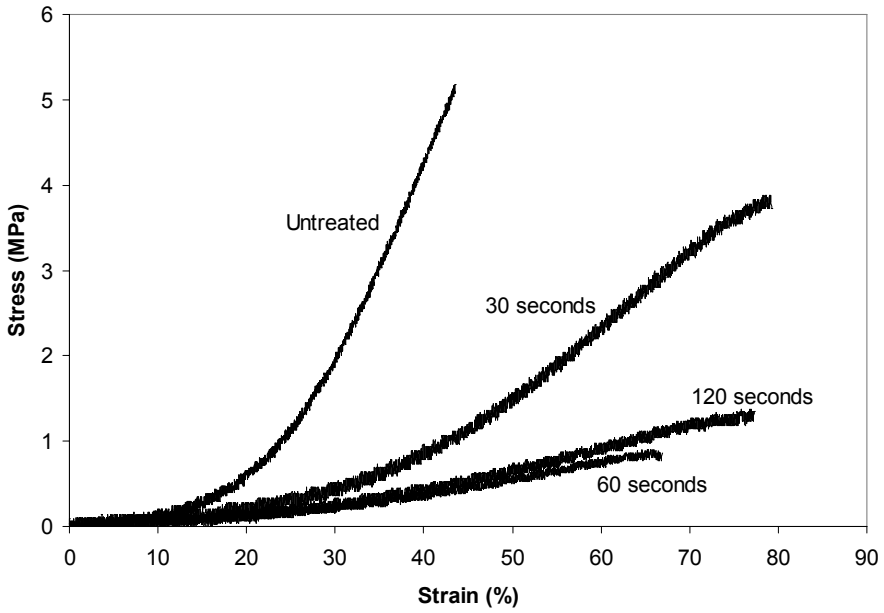

Fig. 5. Typical stress–strain curves from heat-treated and control sample groups. Samples were heated for 30, 60, or 120 s.

We calculated the initial modulus at the low extension part of the curve, as this method has been shown to agree fairly well with the *in vivo* methods of determining the Young's modulus [4]. To calculate the initial modulus we fit a fourth-order polynomial to each curve and extracted the linear term from the best fit line. We also calculated the tangent modulus, the slope of the curve after it goes nonlinear. Other research has shown that Young's modulus for human skin varies widely, from 20 kPa to 57 MPa. This variance occurs due to different models used in calculating the modulus, and because skin's properties are often site-dependent [9]. Young's modulus is most accurately determined using tension tests. However, modulus values *in vivo* are typically determined by suction or torsion tests.

Table 1. Young's modulus for heat-treated and untreated pigskin

Sample treatment	Young's modulus (MPa)	
	Initial	Tangent
Untreated	3.3	17
30 s at 100°C	1.7	5.0
60 s at 100°C	0.97	2.0
120 s at 100°C	0.71	2.3

Our values of Young's modulus for pigskin, as shown in Table 1, are on the order of the values determined for human skin. Additionally, the table shows the differences in the sample groups. The control samples have a higher modulus than the heat-treated samples. Increasing the period of elevated temperature appears to decrease Young's modulus, until very little difference is recorded between 60 and 120 s of heat treatment. Research has suggested that stiffness is directly related to collagen cross-links [5, 10]. Thus, heat may break down the cross-

links during the first 60 s, causing the lack of stiffness. If this is the case, once all the cross-links have broken down, additional high-temperature exposure will show little effect on stiffness.

Local versus far-field strain

Digital image correlation was run on many samples to compare local strain with far-field strain. Figure 6 displays the variance in displacement *u* under strain for one sample. The portion of the skin on the left of the figure translated approximately 20.5 microns, while the right portion translated only 16.5 microns. The irregularities in the contour plot may be an indication of the skin's natural irregularities. Since skin is a heterogeneous material, it will react nonuniformly under tension.

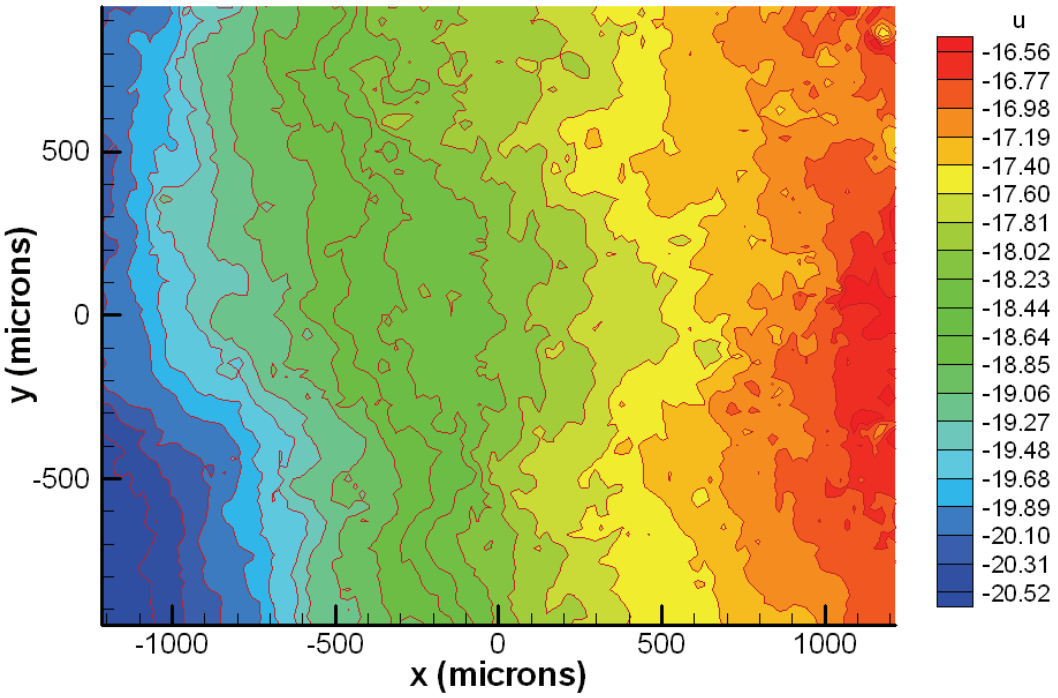

Fig. 6. Contour plot of displacements along the *x* direction using DIC during a uniaxial tension test. Each line corresponds to a 1.2 micron difference with the previous line. The left-to-right grayscale values in the image correspond to the values bottom-to-top in the legend.

We were able to determine strain from the output files of the DIC software. We plotted the stress, as we had determined for our far-field measurements, against the DIC-measured strain. Our results, as shown in Fig. 7, display the similarities and differences between DIC-measured strain and far-field strain. As expected, the strain computed using DIC is less than the far-field strain, as there may be some compliance of our testing apparatus. Additionally, the limits of digital image correlation may have been reached in calculation of strain. Digital imaging can detect only small deformations, as large deformations may cause the image to move out of the field of view. However, the DIC curve does display the characteristic linear extension region, followed by the nonlinear portion.

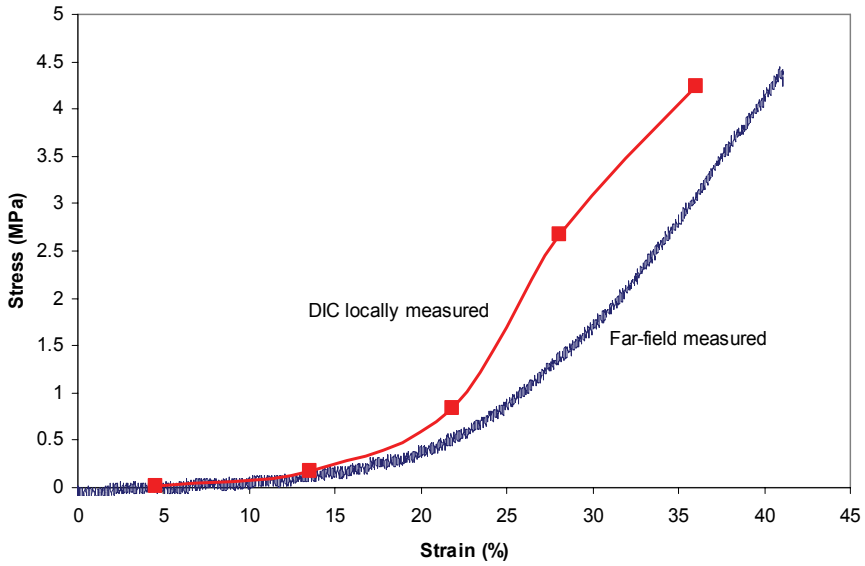

Fig. 7. Stress–strain curve as measured locally by DIC, and as measured at the far-field.

Conclusions

Digital image correlation is a technique developed for use on hard materials and structures. However, its use for biological and soft materials shows promise as well. Image correlation is able to detect small translations and deformation fields of skin. Furthermore, variations in the DIC contour and vector plots reveal the heterogeneous nature of skin. Imaging techniques have their limitations; our DIC software was unable to detect translations accurately below 0.4 microns. Additionally, DIC cannot detect large deformations and translations, as the surface to be correlated may move beyond the field of view.

Research done on the response of heat-treated samples shows that skin becomes less rigid when exposed to elevated temperature. However, a limit is reached where the skin will not become less stiff, even when exposed to longer periods of elevated temperature. We hypothesize that heat breaks down the bonds of the collagen fibers. Once most of the bonds are broken, skin will lose no more rigidity under more exposure to elevated temperature.

It is clear that DIC can prove a suitable method for determining the mechanical properties of skin. Its ability to measure strain fields and translations at the micron scale show promise that DIC may be suitable for measurements of other biological samples. Digital image correlation has possibilities beyond the mechanical realm, in research in the fields of biology, medicine, and industry.

Acknowledgments

The author would like to thank the National Science Foundation for its support of his research under the REU program. The author also acknowledges the Theoretical and Applied Mechanics Department and the Beckman Institute for Advanced Science and Technology at the University of Illinois at Urbana-Champaign for their part in making this research possible. The

author thanks Dr. Matthew Wheeler for providing the pigskin for research. Special thanks are extended to advisors, mentors, and friends for their support, guidance, and instruction during this project.

References

[1] Peters, W. H., W. F. Ranson, M. A. Sutton, T. C. Chu, and J. Anderson. 1983. Application of digital correlation methods to rigid body mechanics. *Optical Engineering* **22**(6), 738–742.

[2] Marcellier, H., P. Vescovo, D. Varchon, P. Vacher, and P. Humbert. 2001. Optical analysis of displacement and strain fields on human skin. *Skin Research and Technology* **7**, 246–253.

[3] Birschoff, J. E., E. M. Arruda, and K. Grosh. 2000. Finite element modeling of human skin using an isotropic, nonlinear elastic constitutive model. *Journal of Biomechanics* **33**(6), 645–652.

[4] Edwards, C., and R. Marks. 1995. Evaluation of biomechanical properties of human skin. *Clinics in Dermatology* **13**, 375–380.

[5] Ankersen, J., A. E. Birbeck, R. D. Thomson, and P. Vanezis. 1999. Puncture resistance and tensile strength of skin simulants. *Proceeding of the Institution of Mechanical Engineers* **213**(H), 493–501.

[6] Foutz, T. L, E. A. Stone, and C. F. Abrams Jr. 1992. Effects of freezing on mechanical properties of rat skin. *American Journal of Veterinary Research* **53**(5), 788–792.

[7] Bruck, H. A., S. R. McNeill, M. A. Sutton, and W. H. Peters III. 1989. Digital image correlation using Newton–Raphson method of partial differential correction. *Experimental Mechanics* **29**, 261–267.

[8] Abanto-Beuno, J. L. 2004. Fracture of a model functionally graded material manufactured from a photo-sensitive polyethylene. Ph.D. dissertation, Department of Aerospace Engineering, University of Illinois at Urbana-Champaign.

[9] Diridollou, S., D. Black, J. M. Lagarde, Y. Gall, M. Berson, V. Vabre, F. Patat, and L. Vaillant. 2000. Sex- and site-dependent variations in the thickness and mechanical properties of human skin *in vivo*. *International Journal of Cosmetic Science* **22**(6), 421.

[10] Dombi, G. W., R. C. Haut, and W. G. Sullivan. Correlation of high-speed tensile strength with collagen content in control and lathyritic rat skin. 1993. *Journal of Surgical Research* **54**(1) 21–28.